Separation Science and Technology
Publication details, including instructions for authors and subscription information:
http://www.informaworld.com/smpp/title~content=t713708471

Effect of Raw Multi-Wall Carbon Nanotubes on Morphology and Separation Properties of Polyimide Membranes

M. A. Aroon[ab]; A. F. Ismail[b]; M. M. Montazer-Rahmati[a]; T. Matsuura[bc]
[a] Membrane Research Laboratory, School of Chemical Engineering, College of Engineering, University of Tehran, Tehran, Iran [b] Advanced Membrane Technology Center (AMTEC), University Teknologi Malaysia, Skudai, Johor Bahru, Malaysia [c] Industrial Membrane Research Laboratory, Department of Chemical and Biological Engineering, University of Ottawa, Ottawa, Ontario, Canada

Online publication date: 29 November 2010

To cite this Article Aroon, M. A. , Ismail, A. F. , Montazer-Rahmati, M. M. and Matsuura, T.(2010) 'Effect of Raw Multi-Wall Carbon Nanotubes on Morphology and Separation Properties of Polyimide Membranes', Separation Science and Technology, 45: 16, 2287 — 2297
To link to this Article: DOI: 10.1080/01496395.2010.484007
URL: http://dx.doi.org/10.1080/01496395.2010.484007

Separation Science and Technology, 45: 2287–2297, 2010

ISSN: 0149-6395 print/1520-5754 online
DOI: 10.1080/01496395.2010.484007

Taylor & Francis
Taylor & Francis Group

Effect of Raw Multi-Wall Carbon Nanotubes on Morphology and Separation Properties of Polyimide Membranes

M. A. Aroon,[1,2] A. F. Ismail,[2] M. M. Montazer-Rahmati,[1] and T. Matsuura[2,3]

[1]*Membrane Research Laboratory, School of Chemical Engineering, College of Engineering, University of Tehran, Tehran, Iran*

[2]*Advanced Membrane Technology Center (AMTEC), University Teknologi Malaysia, Skudai, Johor Bahru, Malaysia*

[3]*Industrial Membrane Research Laboratory, Department of Chemical and Biological Engineering, University of Ottawa, Ottawa, Ontario, Canada*

Raw multi wall carbon nanotubes (r-MWCNTs) were embedded as fillers inside the polyimide (PI) matrix and PI/r-MWCNTs mixed matrix membranes were fabricated by the phase inversion method. The TEM images and permeation results using helium as test gas showed that r-MWCNTs were generally closed ended and acted as impermeable nano particles. Gas permeation tests using CO_2 and CH_4 showed that the addition of r-MWCNTs into the dope solution increased the CO_2/CH_4 separation factor while decreasing the carbon dioxide and methane permeances. When the r-MWCNTs content was increased from 0% to 6 wt.%, permeance of CO_2 in the flat sheet mixed matrix membranes decreased from 9.15 GPU to 5.49 GPU and CO_2/CH_4 separation factor increased from 19.05 to 45.75. Identical to flat sheet mixed matrix membranes, the addition of 2 wt.% r-MWCNTs into a spinning dope increased the CO_2/CH_4 separation factor from 46.61 to 72.20. The glass transition temperature of the mixed matrix flat sheet membranes increased with an increase in the r-MWCNTs content. This implies a good segmental-level attachment between the two phases that forms a rigidified polymer region at the polymer/r–MWCNTs interface. FESEM images showed well dispersed r-MWCNTs in the polymer matrix at a loading of 2 wt% r-MWCNTs.

Keywords gas separation; mixed matrix membranes; multi wall carbon nanotubes

INTRODUCTION

In 1991 Robeson, and later in 1999 Freeman presented a selectivity versus permeability plot and showed that the selectivity of many polymeric membranes for various gas pairs lies on or below a straight line defined as the upper bound tradeoff curve (1,2). To overcome the Robeson's upper bound tradeoff, researchers started to use carbon membranes for the separation of gases (3). Some researchers indicated that these membranes are difficult to handle and expensive to fabricate, fragile, easily plagued by cracks or gaps, and difficult to be transformed into a high surface area module (4,5).

Mixed matrix membranes started to emerge as an alternative in membrane technology. In this approach, superior gas separation properties of molecular sieve materials combine with desirable mechanical properties and economical processability of polymers (6). Zeolites and carbon molecular sieves (CMS) are the most commonly used inorganic fillers for mixed matrix membrane development (5–8). Metal organic frameworks (9), activated carbon (10,11), and carbon nanotubes (12,13) are other types of materials that have been applied as the dispersed phase in mixed matrix membranes fabrication.

Among these materials, carbon nanotubes (CNTs) have been proposed recently for gas separation application due to the following attractive properties (12,14–16):

1. High mechanical strength
2. High strength-to-weight ratio
3. Large length/diameter ratio
4. High thermal stability
5. Very smooth internal surface
6. Precise diameter

Briefly, carbon nanotubes are rolled-up cylinders of graphite sheets (Grapheme) of sp^2 hybridization bonded carbon atoms whose diameter is several Angstroms and whose length is up to several microns (14,17). The nanotubes can be synthesized as singular tubes (single wall carbon nanotubes) or may consist of up to tens or hundreds of co-centric shells of carbon (multi-wall carbon nanotubes).

Due to the aforementioned properties of carbon nanotubes, these tubes are suitable for the preparation of composite materials with high mechanical strength and high thermal stability. In addition, carbon nanotubes have

Received 30 December 2009; accepted 6 April 2010.

Address correspondence to Prof. Ahmed Fauzi Ismail, Advanced Membrane Technology Research Center (AMTEC), University Teknologi Malaysia, 81310 Skudai, Johor Bahru, Johor, Malaysia. E-mail: afauzi@utm.my

been used extensively as field emitters, electro-catalysts of an oxygen reduction reaction, which is important for fuel cells, battery electrodes, high-capacity hydrogen storage media, central elements of electronic devices, logic circuits (14), and adsorption systems (18). Furthermore, due to their smooth surface and their excellent separation properties, carbon nanotubes have also been used as potential new fillers in mixed matrix membranes fabrication (12,15,16,19,20).

Although carbon nanotubes have excellent separation, electrical and mechanical properties, raw carbon nanotubes are a mixture of CNTs on the catalytic support together with amorphous carbon, metal particles, and other carbon nanomaterials (21,22) which must be efficiently eliminated for potential applications. Depending on CNTs morphology and the processes used for the preparation of CNTs, both chemical and physical methods can be used for the purification of carbon nanotubes (23). Chemical methods (such as oxidation by heating, or with acids and oxidizing agents, alkali treatment, and annealing in inert gases) can effectively purify the CNTs but remarkable damages to the nanotubes' morphology and wide loss of product during the purification process may be expected (24). On the other hand, physical methods (such as ultrasonication, filtration, centrifugation, and size-exclusive chromatography) are more complex and less effective compared to the chemical techniques (24).

The objective of this research is to investigate the effect of raw multi-wall carbon nanotubes (r-MWCNTs) on the morphology and separation properties of polyimide membranes. Raw MWCNTs were chosen as fillers to avoid the loss of CNTs and damages to the nanotubes' morphology during the complex purification procedure.

EXPERIMENTAL

Materials

The dope used in this study consisted of polyimide (PI) supplied by A. Johnson Mattey Company, and N-methylpyrrolidone (NMP), tetrahydrofuran (THF), and ethanol (EtOH), supplied by Merck. Tap water was used as the coagulation medium. Multi-wall carbon nanotubes were synthesized using a catalytic chemical vapor deposition (CCVD) system at atmospheric pressure and characterized by the authors.

Fabrication of PI Flat Sheet Membranes

Polyimide flat sheet membranes for gas separation were fabricated using the wet phase inversion method. Polyimide was dried in an oven at 120°C overnight to remove any adsorbed water. Then a predetermined amount of polyimide was added to the solvent mixture gradually and the mixture was stirred for 1 day. After this period of time, the prepared homogeneous viscous polymeric solution was sonicated for 90 minutes and then degassed for 1 day to remove the gas bubbles that may exist in the dope. After degassing, the dope was cast onto a glass plate with a casting knife for a gap setting of 200 micrometers at ambient conditions and was then immediately immersed into the coagulation bath. After 1 day of immersion in water, to remove the remaining solvent, the water in the membrane was replaced by n-hexane following the methanol/n-hexane solvent exchange technique and, subsequently, the membrane was dried (25,26). Furthermore, the membrane so fabricated was coated with silicone rubber using a commercial elastomer product called Sylgard 184. The silicone elastomer was supplied in two parts: a lot-matched base and a curing agent. The coating solution was prepared by thoroughly mixing the base material and the curing agent in a 10:1 by weight ratio and further dilution to 3 wt.% in n-hexane. The membrane was immersed in the coating solution for 6 hours, removed from the coating solution, and left in an oven at 85°C overnight. Table 1 shows the casting conditions.

Fabrication of PI Hollow Fiber Membranes

Asymmetric polyimide hollow fiber membranes for gas separation were fabricated using a dry/wet spinning process.

The dope preparation method for hollow fiber was identical to the flat sheet, as described earlier. After degassing, the polymeric solution was poured slowly into the dope reservoir (500 mL) at ambient temperature. The polymer solution was delivered from the reservoir by a gear pump (Induction Motor 5IK60GU-SF) to the spinneret that was maintained at 10 bar gauge under nitrogen pressure to prevent cavitation in the line to the pump. The bore fluid was pumped to the spinneret using a peristaltic pump (MASTERFLEX 77200-60) simultaneously and the dope and bore fluids were co-extruded through the spinneret as shown in Fig. 1. Tap water at ambient conditions was used as the external coagulant while a mixture of NMP and distilled water (90/10 wt.%) was used as the bore fluid in order to create an open porous inner surface without a skin and minimize substructure and inner skin effects on fiber performance (27–29). The ratio of the dope extrusion

TABLE 1
Polyimide flat sheet membrane fabrication conditions

Casting parameters	Values
Dope composition (wt.%)	PI 25, solvent mixture 75
Solvent mixture composition (wt.%, total sum of 75 wt.%)	NMP 48.2, THF 16.1, EtOH 10.7
Coagulant	Tap water
Coagulation bath temperature	25°C
Ambient conditions	25°C and 84% relative humidity

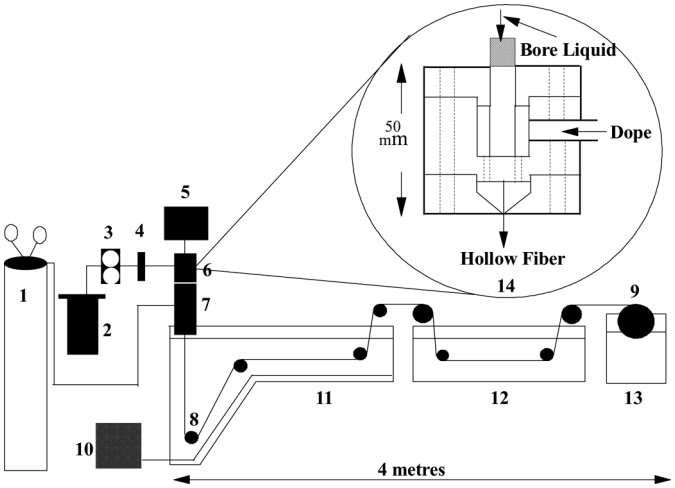

FIG. 1. Schematic diagram of hollow fiber spinning system: (1) nitrogen cylinder; (2) dope reservoir; (3) gear pump; (4) on-line filter, 7 mm; (5) peristaltic pump; (6) spinneret; (7) forced convective tube; (8) roller; (9) wind-up drum; (10) refrigeration/heating unit; (11) coagulation bath; (12) washing/treatment bath; (13) wind-up bath; (14) schematic diagram of the spinneret.

rate to bore fluid injection rate was maintained almost constant at 3.0 in order to reduce the complicated coupling effects of bore fluid on fiber formation. To minimize the effects of elongation stress and gravity on fiber formation, the jet stretch ratio (ratio of drum take-up speed to dope extrusion speed) was kept constant at 1.0 (29). After spinning, the membranes were immersed in water to remove the remaining solvents and then dried using a methanol/n-hexane solvent exchange technique (26,30). The hollow fibers were hung vertically and air-dried at room temperature for 1 day. Similar to flat sheet membranes, hollow fiber membranes were coated by silicon rubber/n-hexane solution as described earlier. Table 2 shows the spinning conditions.

Fabrication of PI/r-MWCNTs Flat Sheet and Hollow Fiber Mixed Matrix Membranes

Except for the dope composition and dope preparation process, other procedures for fabrication of mixed matrix membranes were identical to the neat polymer membranes. The dope preparation procedure of the mixed matrix membrane was as follows. First, raw carbon nanotubes and polyimide were dried in an air circulating oven (Memmert model 100–800) at 120°C overnight. Then a predetermined amount (1–6 wt.%) of raw MWCNTs (r-MWCNTs) was added into the solvent mixture and the resulting suspension was sonicated for 20 minutes for better particle distribution. The suspension was further stirred for 4 hours to separate the particles by the high shear rate (31). After this period of time; polyimide was added gradually into the particle suspension and the polymeric suspension, composed of polyimide and r-MWCNTs in the solvent mixture, was stirred for 1 day to obtain a homogeneous viscous solution. Table 3 shows the mixed matrix membrane dope composition.

Characterization of Flat Sheet Polymeric and Mixed Matrix Membranes

The morphology of polymeric membranes was observed by a low vacuum scanning electron microscope (SEM: JEOL JSM-6390LV) while for characterization of polyimide/r-MWCNTs mixed matrix membranes, a field emission scanning electron microscope (FESEM: JEOL JSM-6701 F) was used. The samples for SEM and FESEM characterization were prepared by breaking membranes after immersion in liquid nitrogen, followed by Pt coating. The structure and properties of raw multi-wall carbon

TABLE 2
Polyimide hollow fiber membrane fabrication conditions

Spinning parameters	Values
Spinneret dimensions	I.D. = 0.55 mm, O.D. = 1.1 mm
Bore fluid flow rate	1 ml/min
Dope flow rate	3 ml/min
Dope flow rate to bore flow rate ratio	3
Jet stretch ratio (ratio of drum take-up speed to dope extrusion speed)	1
Dope composition (wt.%)	PI 25, solvent mixture 75
Solvent mixture composition (wt.%, total sum of 75 wt.%)	NMP 48.2, THF 16.1, EtOH 10.7
Bore fluid composition (wt.%)	NMP 90, distilled water 10
Air gap length	6 cm
Coagulant	Tap water
Coagulation bath temperature	25°C
Ambient conditions	25°C and 84% relative humidity

TABLE 3
The dope composition for the fabrication of PI/r-MWCNTs mixed matrix membranes

Polyimide (wt.%)	Solid base r-MWCNT (wt.%)	Total base r-MWCNT (wt.%)	Solvent mixture (wt.%)	Solvent mixture composition (wt.%)
25	1	0.253	74.747	NMP 48.047, THF 16.02, EtOH 10.68
25	2	0.510	74.490	NMP 47.890, THF 15.96, EtOH 10.64
25	4	1.042	73.958	NMP 47.538, THF 15.85, EtOH 10.57
25	6	1.596	73.404	NMP 47.184, THF 15.73, EtOH 10.49

nanotubes (r-MWCNTs) were examined by a transmission electron microscope (TEM: JEOL JEM-2100). The samples for TEM were prepared by sonication of r-MWCNTs into chloroform and then picking them up on the sample stub surface. The glass transition temperature (T_g) of the samples was measured by a differential scanning calorimeter (DSC: METTLER TOLEDO DSC 822^e).

Gas Permeation Tests

The constant pressure method was used to measure the gas permeation rate as described elsewhere (25). The permeances of the fabricated flat sheet membranes were measured for pure carbon dioxide and methane at 25°C and a feed pressure of 15 bar gauge while fluxes of the hollow fiber membranes were measured for pure carbon dioxide and methane at 25°C and 9 bar gauge. The volumetric flow rate of the permeate was measured by a soap bubble flow meter and converted to the standard temperature and pressure. Each set of data represents 5–10 replicates.

Circular membrane discs with a 5 cm diameter and an effective permeation area of 13.5 cm^2 were used for flat sheet gas permeation tests.

Hollow fiber modules were prepared as follows. Ten fibers were selected and one end was sealed with silicon epoxy (LOCTITE E30-CL HYSOL, USA) to make a hollow fiber bundle. The bundle was then inserted into a stainless steel tube (1/2 inch diameter) and the other end of the bundle was glued to the tube wall with epoxy resin while filling the space between fibers (and the space between the fibers and the wall). This end of the glued bundle was cut with a knife to make the fibers open-ended. The effective length of the fiber was 20 cm. Three to five such modules were tested for each sample in a parallel mode, the feed gas flowed through the shell side channel while permeate flowed through the lumen side channel.

Equation (1) was used to determine the permeance through the membranes:

$$(P/l) = Q/(A \cdot \Delta P) \quad (1)$$

where Q is the measured volumetric flow rate (at standard temperature and pressure), P is the permeability, l is the membrane skin layer thickness, A is the effective membrane area, and ΔP is the pressure difference across the membrane. The common unit of the permeance is GPU and 1 GPU is equal to $10^{-6}\,cm^3(STP)/cm^2 \cdot s \cdot cmHg$.

Equation (2) was used for calculating the ideal separation factor (α):

$$\alpha = P_i/P_j \quad (2)$$

where P_i and P_j are the permeabilities of components i and j, respectively.

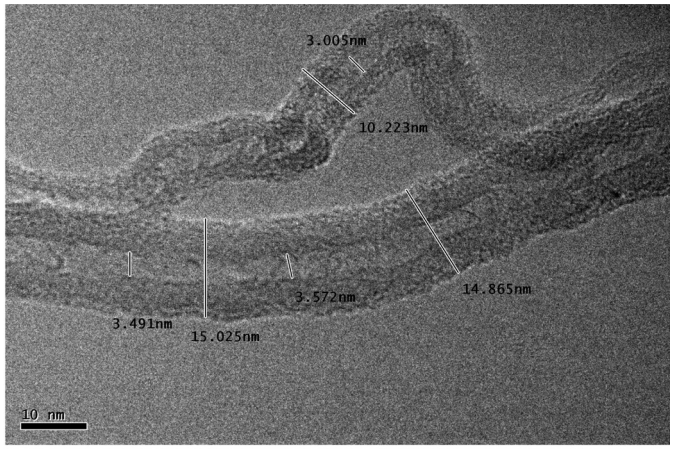

(a)

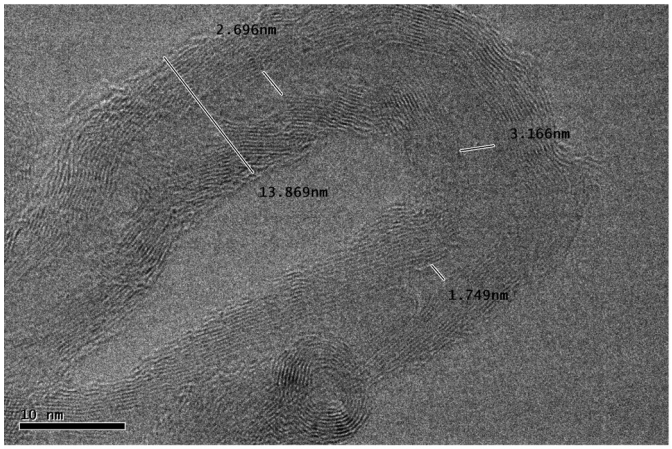

(b)

FIG. 2. Transmission electron microscope images of r-MWCNTs.

RESULTS AND DISCUSSION

Carbon Nanotubes Characterization

Multi-wall carbon nanotubes (MWCNTs) were synthesized by our CNT group using a catalytic chemical vapor deposition (CCVD) system at atmospheric pressure. The supported catalyst (nickel supported on silica-alumina) was prepared by the impregnation method. The reaction was performed at a temperature above 700°C with an optimized reaction time. Acetylene (C_2H_2) was used as the source of carbon for the production of carbon nanotubes (CNTs) and nitrogen (N_2) acted as the carrier gas. The basic mechanism in this process is the dissociation of C_2H_2 molecules catalyzed by the nickel supported on silica-alumina and saturation of carbon atoms in the Ni nano-particles. Precipitation of carbon from the metal particle leads to the formation of carbon nanotubes in a sp^2 structure. The CNT product was collected as a black and fluffy powder. The details of the MWCNTs production technique are given elsewhere (32,33).

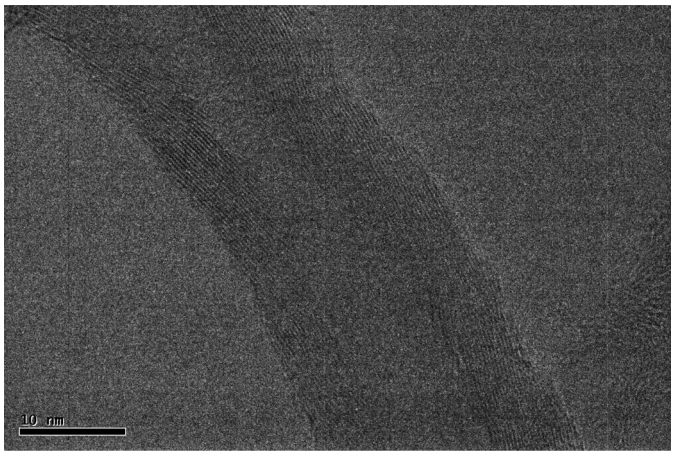

FIG. 3. Amorphous carbon free surface of r-MWCNTs.

The MWCNTs so prepared were used without any further treatment (e.g., purification or functionalization) and are referred to hereafter as r (raw)-MWCNTs.

The TEM images of the r-MWCNTs are shown in Figs. 2a and 2b. The inner diameter of the synthesized multi-wall carbon nanotubes was in the range of 1.75–4.71 nm (average 3.35 nm) and their outer diameter was between 10.22 to 18.44 nm (average 13.8 nm).

Those r-MWCNTs were free from amorphous carbon at the surface as Fig. 3 shows.

The r-MWCNTs were however not pure and catalytic impurity was observed. When the r-MWCNTs were examined, the impurity (black dots) could be detected either

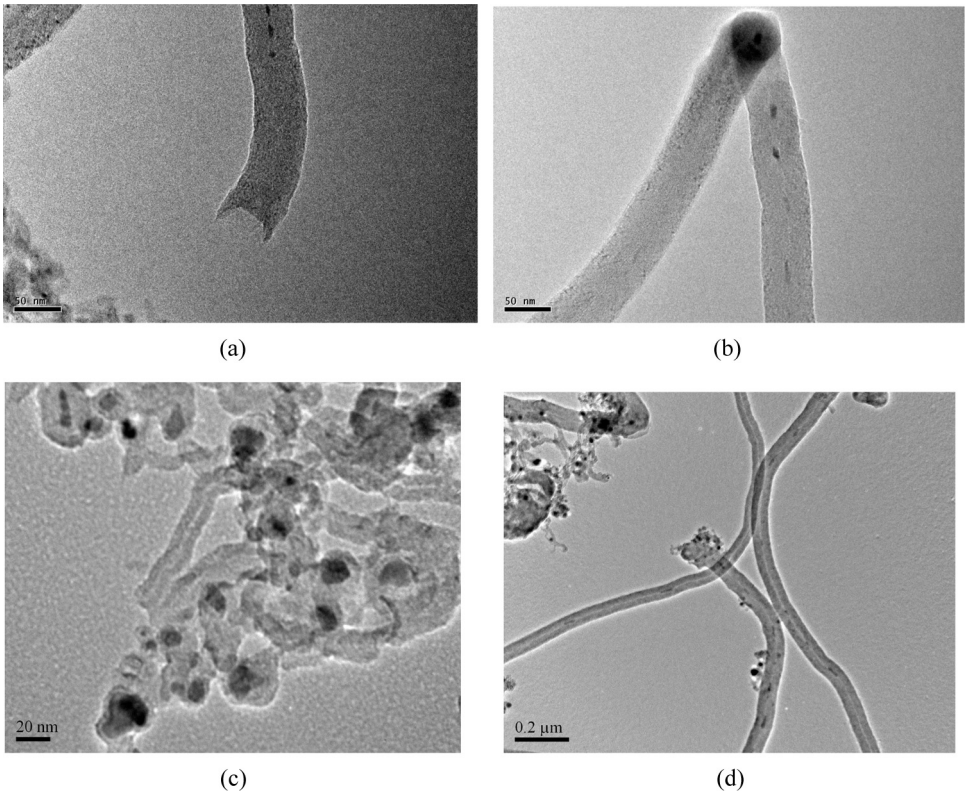

(a) (b)

(c) (d)

FIG. 4. Catalytic impurities on the outer surface, inside or on tips of the r-MWCNTs.

on the outer surface, inside, or on the tips of the carbon nanotubes as shown in Figs. 4a–d. These impurities inside the r-MWCNTs can block penetrants when they are used as fillers in membrane preparation.

In addition to the presence of amorphous carbon and catalytic impurities, the tendency of MWCNTs to agglomerate can affect membrane properties and should be taken into account during dope preparation. Figure 5 is an image of r-MWCNTs in which agglomerated carbon nanotubes are observed.

From these TEM images, it was concluded that most of the carbon-nanotubes are not open cylinders, as evidenced by helium permeation tests discussed later.

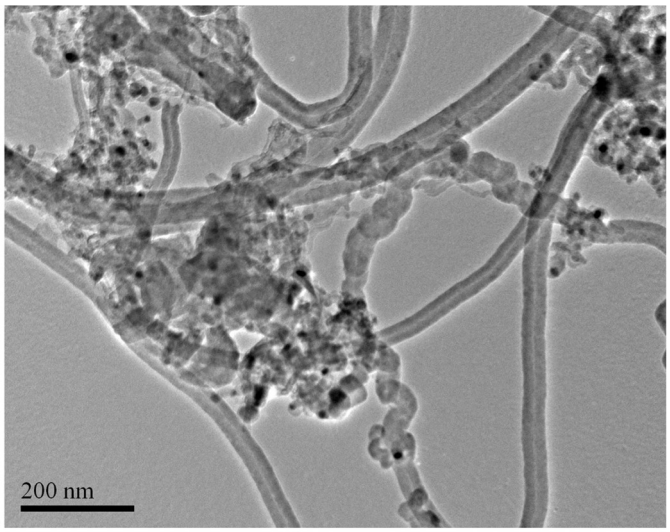

(a)

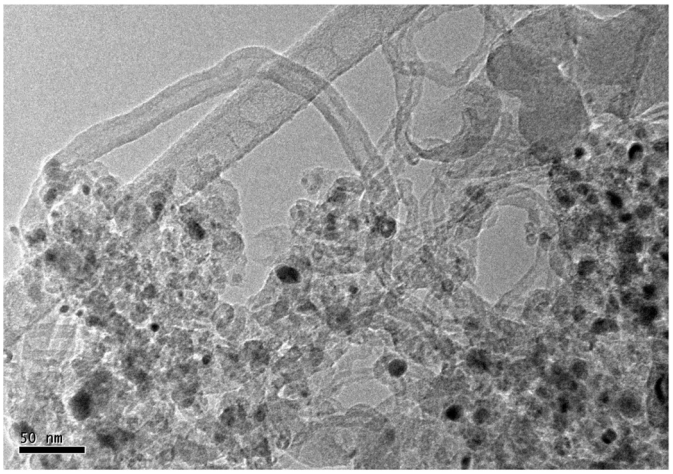

(b)

FIG. 5. TEM images of raw multi walled carbon nanotubes: (a) originally long and endless, (b) agglomerated and blocked by impurities (black dots).

Glass Transition Temperatures of PI and PI/r-MWCNTs Mixed Matrix Flat Sheet Membranes

Addition of a dispersed inorganic phase can affect the fundamental properties (such as T_g) of the polymer matrix when good segmental-level attachment exists between these two phases (6). The glass transition temperature (T_g) is strongly dependent on the thermal, mechanical or processing history of the sample (34). Increased T_g reflects the change in long-range segmental mobility of polymer chains (35). Moore and Koros attributed the T_g increase in the mixed matrix membrane to the rigidification of polymer regions around the particles (36), occurring due to the stresses arising during membrane formation. In the rigidified region, the mobility of polymer chains can be inhibited and the diffusivity difference between larger and smaller gas molecules will possibly increase. Therefore, higher selectivity and lower gas permeability in the vicinity of the dispersed phase will contribute to an improvement in the overall selectivity of the mixed matrix membrane (37).

Table 4 shows the effect of the amount of carbon nanotubes on the glass transition temperature of the flat sheet membranes.

According to Table 4, the glass transition temperature of the neat polyimide flat sheet membrane was about 305.8°C and addition of 1% r-MWCNTs increased the glass transition temperature of the membrane to 318.6°C (by 12.8°C). The glass transition temperature further increased with an increase in r-MWCNTs content. This increase in the glass transition temperature implies a good segmental-level attachment between the two phases as well as the presence of a rigidified polymer region at the polymer/r-MWCNT interface.

Gas Separation Test Results

Gas permeation rates of flat sheet membranes were measured at 15 bar gauge and 25°C using pure carbon dioxide and methane, while gas permeation rates of hollow fiber membranes were measured at 9 bar gauge and 25°C. Table 5 shows the CO_2 and CH_4 permeances of the flat sheet membranes.

TABLE 4
Glass transition temperature of PI and PI/r-MWCNTs mixed matrix flat sheet membranes

Sample description	Solid base r-MWCNTs content in membrane (wt.%)	Glass transition temperature (°C)
Neat polyimide (PI)	0.0%	305.8
PI/r-MWCNTs	1.0%	318.6
PI/r-MWCNTs	2.0%	319.2
PI/r-MWCNTs	6.0%	332.2

TABLE 5
Gas separation properties of PI and PI/r-MWCNTs mixed matrix flat sheet membranes

Sample description	r-MWCNT content in membrane (wt.%)	CO_2 permeance (GPU)	CH_4 permeance (GPU)	CO_2/CH_4 selectivity
Neat polyimide (PI)	0.0	9.15	0.48	19.05
PI-r-MWCNT	1%	8.78	0.38	23.11
PI-r-MWCNT	2%	7.32	0.22	33.26
PI-r-MWCNT	6%	5.49	0.12	45.75

According to Table 5, when the r-MWCNTs content increased from 0% to 6 wt.%, the permeance of CO_2 decreased from 9.15 GPU to 5.49 GPU and the CO_2/CH_4 selectivity increased from 19.05 to 45.75 (by 140%). From the TEM images we have concluded that a large part of the r-MWCNTs are not open-ended cylinders, which can be further supported by helium gas permeation data at 5 bar gauge as follows. Table 6 shows the helium permeation results of PI and PI/r-MWCNTs mixed matrix flat sheet membranes.

As shown in Table 6, the permeance of helium decreased with an increase in r-MWCNTs loading. The decrease in helium permeance can be attributed to the impermeable behavior of r-MWCNTs and to the good adhesion between the dispersed phase and the polymer matrix (12). It is necessary to note that if the r-MWCNTs are open-ended and substantial gas transport takes place in the r-MWCNTs, the results should be the opposite because of the extremely high r-MWCNTs permeability due to their smooth surfaces. Hence, we can conclude that most r-MWCNTs are not open-ended.

Based on this assumption, the permeation data of CO_2 and CH_4 given in Table 5 are interpreted as follows. As mentioned in the foregoing section, the rigidification of the polymer matrix in the presence of r-MWCNTs was proved by T_g measurements. In addition to the rigidification effect, the decrease in the permeance and the increase in the separation factor can be attributed to an increase in the tortuous path around the fillers. Generally, the addition of nonporous particles into the polymer matrix increases the penetrant diffusion pathway length (38,39). Furthermore, although the diffusion pathway length for both penetrants increases, the diffusion rate of the larger molecule through the tortuous path decreases more than the smaller molecule and subsequently the addition of nonporous fillers can improve the separation properties of the resulting mixed matrix membranes (10). Hence, most likely, r-MWCNTs act as impermeable particles and improve the separation properties for gas pairs (CO_2/CH_4) by changing the matrix tortuous pattern. This result is in accordance with the Maxwell model, which predicts that the gas permeability of a mixed-matrix membrane containing nonporous fillers is lower than that of the unfilled polymer and also decreases with increasing filler content (40–42).

Table 7 shows the effect of r-MWCNTs on the performance of mixed matrix hollow fiber membranes.

As shown in Table 7, identical to flat sheet mixed matrix membranes, the addition of r-MWCNTs into the dope can increase CO_2/CH_4 separation factor while CH_4 and CO_2 permeances decrease. Also, an increase in r-MWCNTs loading increases the separation factor of hollow fiber membranes. It is very interesting to note that in contrast to polymer/clay nanocomposites in which a decrease in permeability is not necessarily accompanied by an increase in selectivity (43,44), the addition of only 2 wt.% (solid base) r-MWCNTs into the polyimide matrix can increase the CO_2/CH_4 separation factor by 54.9% (from 46.61 to 72.20).

TABLE 6
Permeance of He in PI and PI/r-MWCNTs mixed matrix flat sheet membranes at 5 bar

Sample description	r-MWCNT content in membrane (wt.%)	He permeance (GPU)
Neat polyimide (PI)	0.0	8.51
PI-r-MWCNT	1%	7.18
PI-r-MWCNT	2%	5.64

Morphology of Mixed Matrix Membranes (SEM and FESEM Results)

Figure 6 shows the cross-sectional SEM images of neat polyimide (PI) and PI/r-MWCNT MMM samples.

TABLE 7
Gas separation properties of hollow fiber membranes

Sample description	Air gap (cm)	CO_2 permeance (GPU)	CH_4 permeance (GPU)	CO_2/CH_4 selectivity
Neat polyimide	6	10.72	0.23	46.61
PI-1% r-MWCNT	6	7.45	0.13	57.31
PI-2% r-MWCNT	6	3.61	0.05	72.20

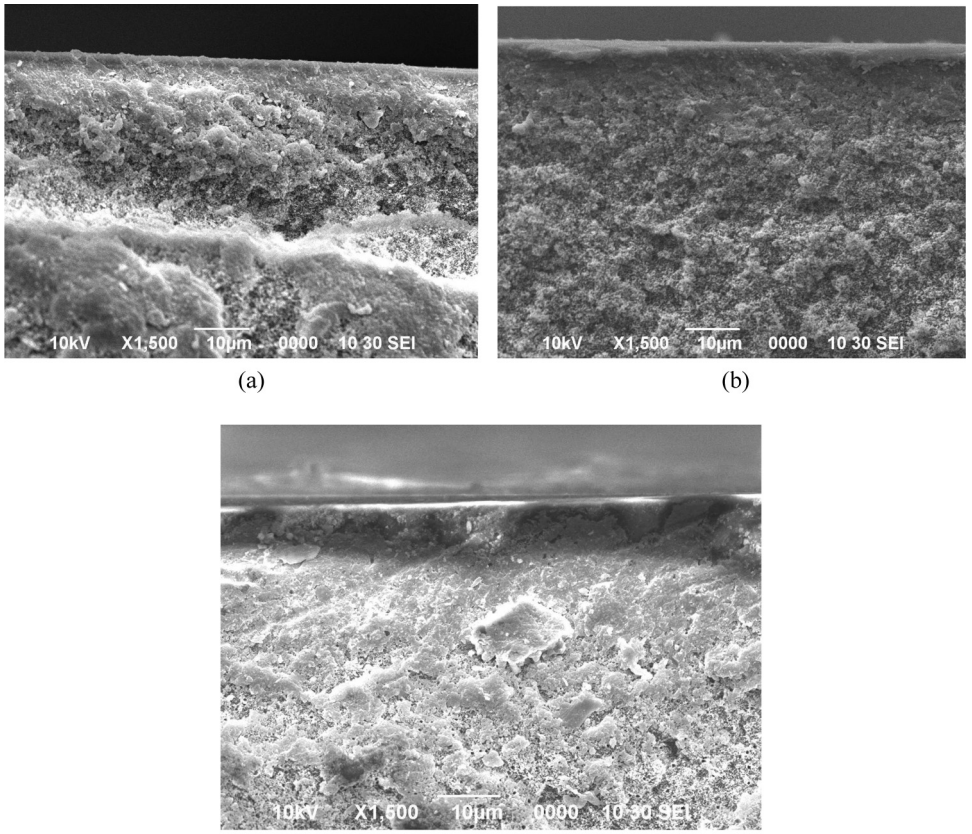

FIG. 6. Cross-sectional SEM images of PI and PI/r-MWCNTs mixed matrix flat sheet membranes; (a): PI, (b): 1% r-MWCNTs embedded in PI, (c): 2% r-MWCNTs embedded in PI.

From Fig. 6 it is found that the structure of the sub-layer was not affected by the addition of r-MWCNT particles. This result is different from Aerts et al.'s (45) and Zhang et al.'s observation (46). This phenomenon can be attributed to the negligible amount of embedded carbon nanotubes. Under this condition, the amount of particles in the casting solution is not enough to hinder their free movement in membrane formation (46).

Although the sub-layer structure did not change, the skin layer thickness (ℓ) decreased as the amount of MWCNTs in the membrane increased (Fig. 7).

This implies that the addition of r-MWCNT particles into the casting solution has an effect on the membrane formation mechanism during the immersion precipitation process. It is likely that the addition of nano-sized particles into the dope increases polymer-particle-polymer interactions, causing the macromolecules to approach the most tightly-coiled conformation. The densification of macromolecules in the skin layer, when it occurs in the vertical direction, makes the skin layer thinner. A decrease in the skin layer thickness, however, does not compensate the rigidification and other effects, and the permeance decreases with an increase in the r-MWCNT content. It is known that adding fillers to the polymer solution results in a mechanically more rigid system, which is also beneficial to forming a porous sub-layer with less macrovoids (46). Further investigation is necessary to prove this mechanism.

In order to investigate the distribution of r-MWCNTs within the polymer matrix, cross-sectional images of the mixed matrix membranes (MMMs) were taken by FESEM.

FESEM images did not reveal r-MWCNTs in the skin layer of the PI/1% and 2% r-MWCNTs mixed matrix flat sheet membranes. This was probably because the nano-sized particles were hidden in the dense structure of the skin layer.

Figure 8 presents the FESEM image (magnification 50,000 x) of the sublayer immediately below the skin layer of a mixed matrix flat sheet membrane with 2 wt.% raw MWCNTs.

Figure 8 shows that some r-MWCNTs are well dispersed in the polymer matrix. Unfortunately, the detailed structure of the r-MWCNTs-polymer matrix interface could not be observed.

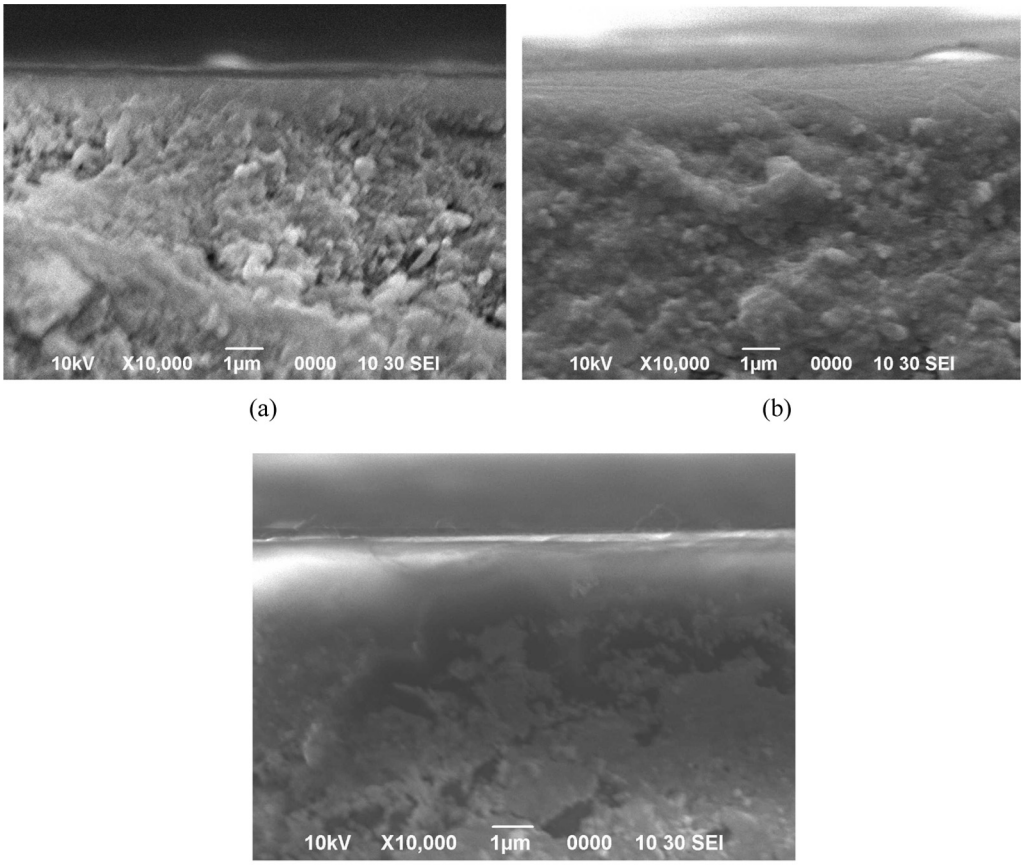

FIG. 7. SEM images of the skin layers of neat PI and PI/r-MWCNTs mixed matrix flat sheet membranes; (a): PI, (b): 1% r-MWCNTs embedded in PI, (c): 2% r-MWCNTs embedded in PI.

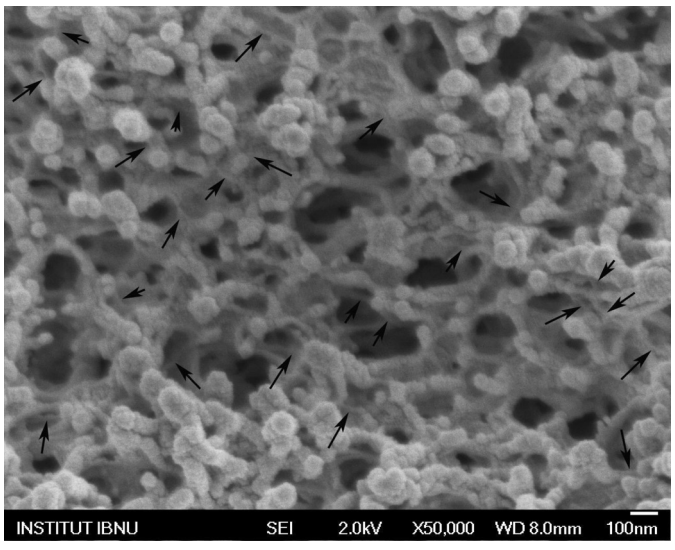

FIG. 8. FESEM images of the sub layer near the skin layer of PI/ 2% r-MWCNTs mixed matrix flat sheet membrane (arrows show the r-MWCNTs).

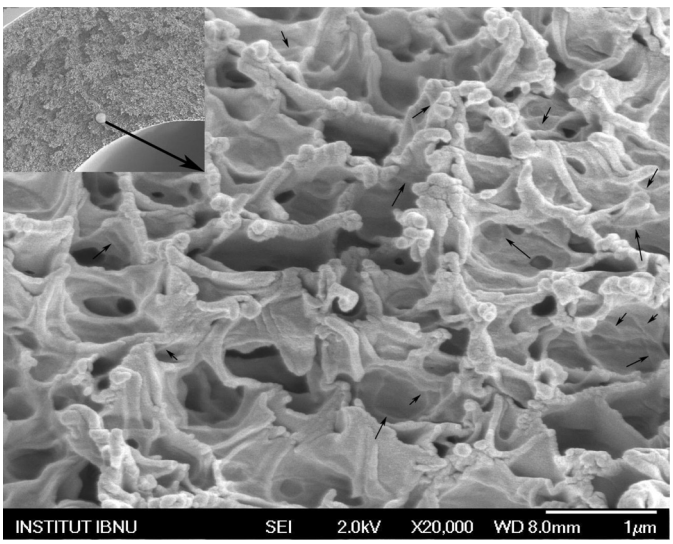

FIG. 9. FESEM images of the inner layer of PI/ 2% r-MWCNTs mixed matrix hollow fiber membrane (arrows show the r-MWCNTs).

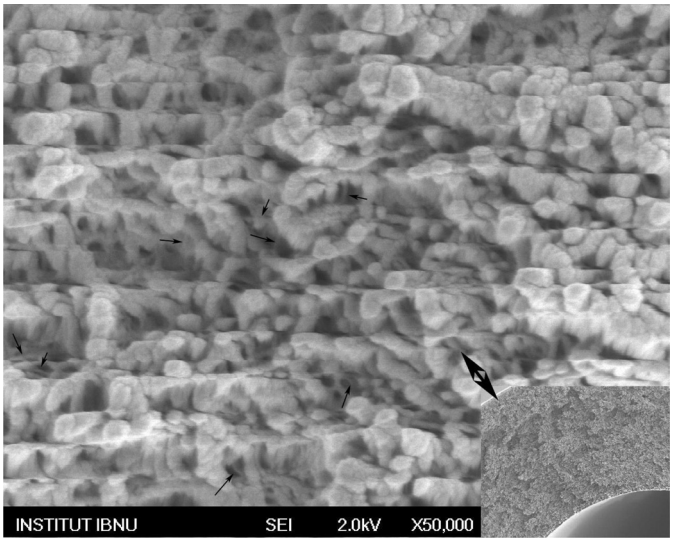

FIG. 10. FESEM images of the sub layer near the skin layer of PI/ 2% r-MWCNTs mixed matrix hollow fiber membrane (arrows show the r-MWCNTs).

Figure 9 presents the FESEM image (magnification 20,000 x) of the sub-layer near the inner layer of a mixed matrix hollow fiber membrane with 2 wt.% raw MWCNTs.

As shown in Fig. 9, some r-MWCNTs dispersed in the polyimide matrix are observed.

Figure 10 shows the FESEM image (magnification 50,000 x) of the sub-layer immediately below the skin layer of a mixed matrix hollow fiber membrane with 2 wt.% raw MWCNTs.

Figure 10 shows some relatively well dispersed raw multi-walled carbon nanotubes in the nodular structure of the sub-layer near the skin layer of the mixed matrix hollow fiber membrane samples.

CONCLUSIONS

Mixed matrix flat sheet and hollow fiber membranes containing raw multi-wall carbon nanotubes (r-MWCNTs) embedded in the polyimide matrix were prepared successfully. The decrease in permeance of CO_2 and CH_4 along with the increase in selectivity for the CO_2/CH_4 gas pair with an increase in r-MWCNTs loading indicates that the addition of supposedly closed-ended raw carbon nanotubes into the dope can increase the tortuous path length of gas molecules in the polymer matrix. This result is in accordance with the Maxwell model which predicts that the gas permeability of the mixed-matrix membrane (MMM) containing nonporous fillers is lower than that of the unfilled polymer. It is also very interesting to note that the addition of only 6 wt.% (solid base) of r-MWCNTs into the polyimide matrix could increase the selectivity for the CO_2/CH_4 gas pair by 140% as compared to the neat PI flat sheet membrane. In other words, a negligible amount of carbon nanotubes could change the separation properties of the fabricated MMMs drastically. In addition to changing the matrix tortuous pattern, the addition of carbon nanotubes into the polymer matrix affected the fundamental properties (such as the T_g) of the polymer matrix. An increase in the glass transition temperature of the flat sheet MMMs with an increase in r-MWCNTs loading implies a good segmental-level attachment between the two phases along with the formation of a rigidified polymer region at the polymer/r-MWCNT interface. The cross-sectional FESEM images of MMMs showed that r-MWCNTs were well-dispersed in the polymer matrix at a loading of 2 wt.%. Also, the SEM results showed that the sub-layer structure of the as-cast flat sheet MMMs did not change with the addition of r-MWCNTs but the skin layer of the MMMs was thinner than that of the neat polyimide flat sheet membrane. This implies that the addition of nano-sized particles into the dope may increase polymer-particle-polymer interactions, leading to a more tightly coiled conformation of the polymer.

ACKNOWLEDGEMENTS

This research was supported by grant number 087125 from the National Iranian Gas Company.

REFERENCES

1. Robeson, L.M. (1991) Correlation of separation factor versus permeability for polymeric membranes. *J. Membr. Sci.*, 62: 165.
2. Freeman, B.D. (1999) Basis of permeability/selectivity trade-off relations in polymeric gas separation membranes. *Macromolecules*, 32: 375.
3. Pabby, A.K.; Rizvi, Syed S.H.; Sastre, A.M. (2009) *Handbook of Membrane Separations Chemical, Pharmaceutical, Food, and Biotechnological Applications*; CRC Press: Boca Raton, FL.
4. Vu, De Q.; Koros, W.J.; Miller, S.J. (2003) Mixed matrix membranes using carbon molecular sieves, I. Preparation and experimental results. *J. Membr. Sci.*, 211: 311.
5. Vu, De Q.; Koros, W.J.; Miller, S.J. (2003) Mixed matrix membranes using carbon molecular sieves II. Modeling permeation behavior. *J. Membr. Sci.*, 211: 335.
6. Moore, T.T.; Mahajan, R.; Vu, De Q.; Koros, W.J. (2004) Hybrid membrane materials comprising organic polymers with rigid dispersed phases. *AIChE J.*, 50: 311.
7. Jiang, L.Y.; Chung, T.S.; Cao, C.; Huang, Z.; Kulprathipanja, S. (2005) Fundamental understanding of nano-sized zeolite distribution in the formation of the mixed matrix single- and dual-layer asymmetric hollow fiber membranes. *J. Membr. Sci.*, 252: 89.
8. Pechar, T.W.; Kim, S.; Vaughan, B.; Marand, E.; Tsapatsis, M.; Jeong, H.K.; Cornelius, C.J. (2006) Fabrication and characterization of polyimide–zeolite L mixed matrix membranes for gas separations. *J. Membr. Sci.*, 277: 195.
9. Zhang, Y.; Musselman, I.H.; Ferraris, J.P.; Balkus, Jr., K.J. (2008) Gas permeability properties of Matrimid® membranes containing the metal-organic framework Cu–BPY–HFS. *J. Membr. Sci.*, 313: 170.
10. Bertelle, S.; Gupta, T.; Roizard, D.; Vallières, C.; Favre, E. (2006) Study of polymer-carbon mixed matrix membranes for CO_2 separation from flue gas. *Desalination*, 199: 401.

11. Anson, M.; Marchese, J.; Garis, E.; Ochoa, N.; Pagliero, C. (2004) ABS copolymer-activated carbon mixed matrix membranes for CO_2/CH_4 separation. *J. Membr. Sci.*, 243: 19.
12. Kim, S.; Pechar, T.W.; Marand, E. (2006) Poly(imide siloxane) and carbon nano tube mixed matrix membranes for gas separation. *Desalination*, 192: 330.
13. Kim, S.; Chen, L.; Johnson, J.K.; Marand, E. (2007) Polysulfone and functionalized carbon nanotube mixed matrix membranes for gas separation: Theory and experiment. *J. Membr. Sci.*, 294: 147.
14. Popov, V. (2004) Carbon nanotubes: properties and application. *Mater. Sci. Eng., A.*, 43: 61.
15. Skoulidas, A.I.; Ackerman, D.M.; Johnson, J.K.; Sholl, D.S. (2002) Rapid transport of gases in carbon nanotubes. *Phys. Rev. Lett.*, 89: 185901/1.
16. Ackerman, D.M.; Skoulidas, A.I.; Sholl, D.S.; Johnson, J.K. (2003) Diffusivities of Ar and Ne in carbon nanotubes. *Mol. Simul.*, 29: 677.
17. Dresselahaus, M.S.; Dresselahaus, G.; Saito, R. (1995) Physics of carbon nanotubes. *Carbon*, 33: 883.
18. Hilding, J.M. (2004) Characterization and applications of multi walled carbon nanotubes. Ph.D. Thesis, The University of Kentucky.
19. Hinds, B.J.; Chopra, N.; Rantell, T.; Andrews, R.; Gavalas, V.; Bachas, L.G. (2004) Aligned multi walled carbon nanotube membranes. *Science*, 303: 62.
20. Chen, H.; Sholl, D.S. (2006) Predictions of selectivity and flux for CH_4/H_2 separations using single walled carbon nanotubes as membranes. *J. Membr. Sci.*, 269: 152.
21. Hou, P.X.; Bai, S.; Yang, Q.H.; Liu, C.; Cheng, H.M. (2002) Multi-step purification of carbon nanotubes. *Carbon*, 40: 81.
22. Liu, Y.; Gao, L.; Sun, J.; Zheng, S.; Jiang, L.; Wang, Y.; Kajiura, H.; Li, Y.; Noda, K. (2007) A multi-step strategy for cutting and purification of single-walled carbon nanotubes. *Carbon*, 45: 1972.
23. Li, J.; Zhang, Y. (2005) A simple purification for single-walled carbon nanotubes. *Physica E: Low-Dimensional Systems and Nanostructures*, 28: 309.
24. Ismail, A.F.; Goh, P.; Tee, J.C.; Sanip, S.M. (2008) A review of purification techniques for carbon nanotubes. *Nano*, 3: 127.
25. Ismail, A.F.; Lai, P.Y. (2003) Effects of phase inversion and rheological factors on formation of defect-free and ultrathin-skinned asymmetric polysulfone membranes for gas separation. *Sep. Purif. Technol.*, 33: 127.
26. Lib, D.F.; Chung, T.S.; Wang, R.; Liu, Y. (2002) Fabrication of fluoropolyimide/polyethersulfone (PES) dual-layer asymmetric hollow fiber membranes for gas separation. *J. Membr. Sci.*, 198: 211.
27. Chung, T.S.; Teoh, S.K.; Hu, X. (1997) Formation of ultrathin high-performance polyethersulfone hollow-fiber membranes. *J. Membr. Sci.*, 133: 161.
28. Wallace, D.W.; Staudt-Bickel, C.; Koros, W.J. (2006) Efficient development of effective hollow fiber membranes for gas separations from novel polymers. *J. Membr. Sci.*, 278: 92.
29. Qin, J.; Chung, T.S. (1999) Effect of dope flow rate on the morphology, separation performance, thermal and mechanical properties of ultrafltration hollow fiber membranes. *J. Membr. Sci.*, 157: 35.
30. Chung, T.S.; Qin, J.J.; Gu, J. (2000) Effect of shear rate within the spinneret on morphology, separation performance and mechanical properties of ultrafiltration polyethersulfone hollow fiber membranes. *Chem. Eng. Sci.*, 55: 1077.
31. Jiang, Y.L.; Chung, T.S.; Kulprathipanja, S. (2006) An investigation to revitalize the separation performance of hollow fibers with a thin mixed matrix composite skin for gas separation. *J. Membr. Sci.*, 276: 113.
32. Tee, J.C.; Ismail, A.F.; Aziz, M.; Soga, T. (2009) Influence of catalyst preparation on synthesis of multi-walled carbon nanotubes. *IEICE Trans*, (in press).
33. Tee, J.C.; Aziz, M.; Ismail, A.F. (2008) Effect of reaction temperature and flow rate of precursor on formation of multi-walled carbon nanotubes. *Journal Teknologi*, 49: 141.
34. Ahn, J.; Chung, W.J.; Pinnau, I.; Guiver, M.D. (2008) Polysulfone/silica nanoparticle mixed-matrix membranes for gas separation. *J. Membr. Sci.*, 314: 123.
35. Moaddeb, M.; Koros, W.J. (1997) Gas transport properties of thin polymeric membranes in the presence of silicon dioxide particles. *J. Membr. Sci.*, 125: 143.
36. Moore, T.T.; Koros, W.J. (2005) Non-ideal effects in organic–inorganic materials for gas separation membranes. *J. Mol. Struct.*, 739: 87.
37. Chung, T.S.; Jiang, L.Y.; Li, Y.; Kulprathipanja, S. (2007) Mixed matrix membranes (MMMs) comprising organic polymers with dispersed inorganic fillers for gas separation. *Prog. Polym. Sci.*, 32: 483.
38. Merkel, T.C.; Freeman, B.D.; Spontak, R.J.; He, Z.; Pinnau, I.; Meakin, P.; Hill, A.J. (2003) Sorption, transport, and structural evidence for enhanced free volume in poly(4-methyl-2-pentyne)/fumed silica nanocomposite membranes. *Chem. Mater.*, 15: 109.
39. DeRocher, J.P.; Gettelfinger, B.T.; Wang, J.; Nuxoll, E.E.; Cussler, E.L. (2005) Barrier membranes with different sizes of aligned flakes. *J. Membr. Sci.*, 254: 21.
40. Polotskaya, G.A.; Andreeva, D.V.; Elyashevich, G.K. (1999) Investigation of gas diffusion through films of fullerene-containing poly (phenylene oxide). *Tech. Phys. Lett.*, 25: 555.
41. Chung, T.S.; Chan, S.S.; Wang, R.; Lu, Z.; He, C. (2003) Characterization of permeability and sorption in Matrimid/C_{60} mixed matrix membranes. *J. Membr. Sci.*, 211: 91.
42. Higuchi, A.; Yoshida, T.; Imizu, T.; Mizoguchi, K.; He, Z.; Pinnau, I.; Nagai, K.; Freeman, B.D. (2000) Gas permeation of fullerene-dispersed poly(1-trimethylsilyl-1-propyne) membranes. *J. Polym. Sci., Part B: Polym. Phys.*, 38: 1749.
43. Choudalakis, G.; Gotsis, A.D. (2009) Permeability of polymer/clay nanocomposites: A review. *Eur. Polym. J.*, 45: 967.
44. Rubal, M.; Wilkins, C.W.; Cassidy, P.E.; Lansford, C.; Yamada, Y. (2008) Fluorinated polyimide nanocomposites for CO_2/CH_4 separation. *Polym. Adv. Technol.*, 19: 1033.
45. Aerts, P.; Van Hoof, E.; Leysen, R.; Vankelecom, I.F.J.; Jacobs, P.A. (2000) Polysulfone – Aerosil composite membranes: Part 1. The influence of the addition of Aerosil on the formation process and membrane morphology. *J. Membr. Sci.*, 176: 63.
46. Zhang, Y.; Li, H.; Lin, J.; Li, R.; Liang, X. (2006) Preparation and characterization of zirconium oxide particles filled acrylonitrile-methyl acrylate-sodium sulfonate acrylate copolymer hybrid membranes. *Desalination*, 192: 198.